Observational limits on the gas mass of a $z = 4.9$ galaxy

R. C. Livermore[1], A. M. Swinbank[1], Ian Smail[1], R. G. Bower[1], K. E. K. Coppin[1,2], R. A. Crain[3], A. C. Edge[1], J. E. Geach[1,2], and J. Richard[1,4]

ABSTRACT

We present the results of a search for molecular gas emission from a star-forming galaxy at $z = 4.9$. The galaxy benefits from magnification of $22\pm5\times$ due to strong gravitational lensing by the foreground cluster MS1358+62. We target the CO(5–4) emission at a known position and redshift from existing *Hubble Space Telescope/ACS* imaging and Gemini/NIFS [OII]3727 imaging spectroscopy, and obtain a tentative detection at the $4.3\,\sigma$ level with a flux of $0.104\pm0.024\,\mathrm{Jy\,km\,s^{-1}}$. From the CO line luminosity and assuming a CO-to-H_2 conversion factor $\alpha = 2$, we derive a gas mass $M_{\rm gas} \sim 1^{+1}_{-0.6} \times 10^9\,\mathrm{M_\odot}$. Combined with the existing data, we derive a gas fraction $M_{\rm gas}/\left(M_{\rm gas} + M_*\right) = 0.59^{+0.11}_{-0.06}$. The faint line flux of this galaxy highlights the difficulty of observing molecular gas in representative galaxies at this epoch, and suggests that routine detections of similar galaxies in the absence of gravitational lensing will remain challenging even with ALMA in full science operations.

Subject headings: galaxies: high-redshift — galaxies: star formation — gravitational lensing: strong

1. Introduction

Extensive studies of optically-selected star-forming galaxies seen at the epoch of peak cosmic star-formation density ($z \sim 2$) have revealed star-formation rates (SFRs) of 10-100 $\mathrm{M_\odot yr^{-1}}$ and stellar masses of $\sim10^{10-11}\mathrm{M_\odot}$ (e.g. Förster Schreiber et al. 2009; Law et al. 2009; Tacconi et al. 2010; Daddi et al. 2010b). If these SFRs have been continously maintained, then these galaxies must have undergone their first major epoch of stellar mass

[1]Institute for Computational Cosmology, Durham University, South Road, Durham DH1 3LE, UK

[2]Department of Physics, McGill University, 3600 rue University, Montréal, QC H3A 2T8, Canada

[3]Leiden Observatory, Leiden University, PO Box 9513, 2300 RA Leiden, The Netherlands

[4]CRAL, Observatoire de Lyon, 9 Avenue Charles André, 69561 Saint-Genis-Laval, France

assembly 1–2 Gyr earlier, at $z \sim 5$, when the bulk of the star-forming population was $\sim 5\times$ less massive (McLure et al. 2009; Stark et al. 2010).

The star formation within these galaxies is fuelled by reservoirs of predominantly cold molecular hydrogen, H_2. Since the H_2 is not directly detectable, CO emission at millimetre wavelengths has been employed to trace the cold molecular gas. However, exploring gas properties of galaxies beyond $z \sim 3$, is challenging; not only does the apparent surface brightness reduce as $(1+z)^{-4}$, but the galaxies themselves also appear systematically smaller and intrinsically fainter making detections of their molecular gas emission difficult.

To date, studies of molecular line emission at $z > 3$ have been limited to extreme populations such as gas-rich quasars (e.g. Walter et al. 2009) and submillimetre galaxies (SMGs; Coppin et al. 2010; Carilli et al. 2010; Riechers et al. 2011a). Detecting typical star-forming galaxies at $z > 3$ has proven difficult because the CO line luminosities are usually below the sensitivity limits of current facilities (Stanway et al. 2008; Davies et al. 2010).

However, it is still possible to study less active high-z galaxies which are strongly gravitationally lensed by massive galaxy clusters. The magnification provided by gravitational lensing has enabled detections of molecular gas in a number of star-forming galaxies up to $z \sim 3$ (e.g. Baker et al. 2004; Coppin et al. 2007; Riechers et al. 2011b; Danielson et al. 2011), and more recently $z \sim 4-6$ (e.g. Cox et al. 2011; Combes et al. 2012). The physical properties of the interstellar medium appear similar to those in local ULIRGs, with high gas fractions, high densities and intense UV radiation fields.

Franx et al. (1997) reported the detection of a multiply-imaged $z = 4.9$ galaxy which is gravitationally lensed by the massive galaxy cluster MS 1358+62. Correcting for lensing, this galaxy (hereafter MS1358-arc) appears to be representative of the star-forming population at this epoch (its lensing-corrected apparent magnitude is I_{AB}=24.9, marginally brighter than the characteristic luminosity of $I_{AB} = 25.3$ at $z \sim 5$; Ouchi et al. 2004). Swinbank et al. (2009, hereafter S09) carried out a detailed study of one image of the MS1358-arc system, using optical and infrared imaging combined with integral field spectroscopy, revealing a rotating system across 2 kpc in projection, with star formation occuring in five bright clumps.

In this Letter, we report observations with the Plateau de Bure Interferometer to search for CO(5-4) emission in MS1358-arc. Throughout, we adopt a ΛCDM cosmology with $H_0 = 70\,\mathrm{km\,s^{-1}\,Mpc^{-1}}$, $\Omega_\Lambda = 0.7$ and $\Omega_m = 0.3$.

2. Observations and Data Reduction

The MS1358+62 system is illustrated in Figure 1, with the positions of the two images of MS1358-arc marked (Table 1). We estimate the amplification of each image using the lens model of Richard et al. (2008) with `lenstool` (Kneib 1993; Jullo et al. 2007), with errors accounting for the magnification gradient across the image. The combined magnification factor for Image 1 and 2 is $\mu = 22 \pm 5$.

To search for the CO(5–4) emission, we observed MS1358-arc with the IRAM Plateau de Bure Interferometer (PdBI; Guilloteau et al. 1992), using six antennae in D (compact) configuration. The pointing centre was $\alpha_{2000}, \delta_{2000} = 13:59:48.7, +62:30:48.34$, and the frequency was tuned to the CO(5–4) transition (rest frame 576.2679 GHz) redshifted to 97.185 GHz (based on the [OII]-derived systemic redshift of $z = 4.9296 \pm 0.0002$ from S09). The observations were made between 2010 June 4 and 2010 June 6 with total on-source time of 10 hours, using WIDEX with a resolution of 2.5 MHz. The star MWC349 was observed as the primary flux calibrator, with the quasars 1749+096, 0923+392 and 2145+067 as secondary flux calibrators. Receiver bandpass calibration was performed against 0923+392 and 3C454.3, and 1435+638 and 1418+546 were used for phase and amplitude calibration.

The data were reduced with the `gildas` software package (Guilloteau & Lucas 2000) and resampled to a velocity resolution of 38.6 km s^{-1}. The synthesised beam is a Gaussian ellipse with a FWHM size of $5.6 \times 4.3''$ at a position angle of 111°.

The PdBI observations were centered on the two brightest images of the $z \sim 5$ galaxy. The images are both within 6" of the pointing centre, whereas the primary beam of PdBI at 3mm is 50"; we have therefore not corrected for primary beam attenuation, which is negligible. First, we construct a channel map from a 90km s^{-1} window around the CO(5–4) emission line centered at the systemic redshift, and show as an inset in Figure 1, with contours at $\pm 1\sigma$ intervals. The positions of the images within the PdBI cube are determined by aligning the cube with the *HST* image and taking the centre of the corresponding pixels.

We also extract spectra from these positions and show these in Figure 2. Individually, the two images are clearly extremely faint; by comparing the $\Delta\chi^2$ of a Gaussian profile to that of a continuum-only fit, measuring the noise over a 1200 km s^{-1} channel, the significances of the CO(5–4) emission lines in Images 1 and 2 are 3.3σ and 2.7σ respectively. However, since they are separated by more than one beam width, we can improve the signal to noise by coadding the spectra at the two positions using uniform weights (Figure 2); we then obtain a 1σ rms channel sensitivity of 0.4 mJy per 38.6 km s^{-1} channel. Again comparing the χ^2 of a Gaussian profile fit to that of a continuum-only fit, we use the $\Delta\chi^2$ to derive a significance level of $4.3\,\sigma$ for the coadded CO(5–4) emission line.

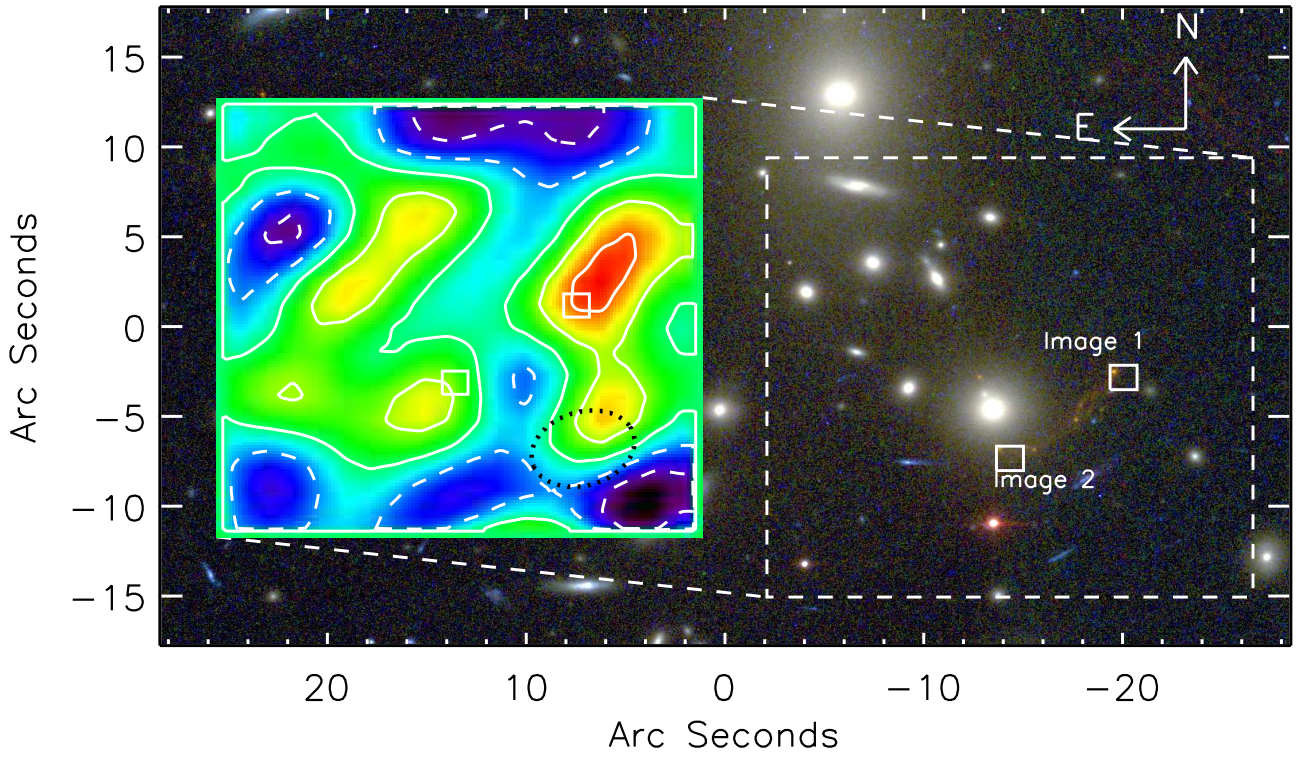

Fig. 1.— *Hubble Space Telescope (HST)/ACS* image of the core of MS1358+62. The squares mark the extent of the pixels in the PdBI cube used to extract the spectra shown in Figure 2. A Plateau de Bure channel map constructed from a 90km s^{-1} window around the systemic velocity of the CO(5-4) line is shown as an inset. The PdBI synthesised beam size is indicated by the dotted ellipse in the inset. Contours are shown in $\pm 1\sigma$ intervals, with negative contours indicated by dashed lines. The origin of the *HST* image coordinate system is $(\alpha_{2000}, \delta_{2000}) = (13^h59^m51.4^s, +62°30'52.5'')$.

Table 1: Positions of the three images of MS1358-arc within the Plateau de Bure field of view and the mean linear magnification factor (μ). The position of the third image is included for completeness, but is excluded from our analysis as it lies outside the primary beam.

Image	RA (J2000)	Dec (J2000)	μ
Image 1	$13^h59^m48.684^s$	$62°30'48.54''$	12.4 ± 3
Image 2	$13^h59^m49.430^s$	$62°30'45.13''$	9.5 ± 4
Image 3	$13^h59^m54.746^s$	$62°31'5.21''$	2.9 ± 0.1

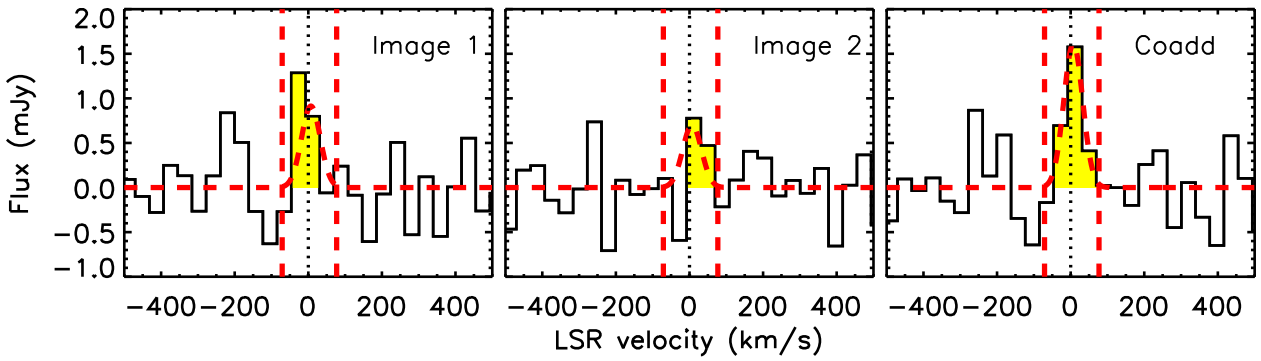

Fig. 2.— The CO(5–4) spectra extracted from the two images of MS1358-arc and the coadd of these spectra. The velocity scale is centered on the systemic redshift $z = 4.9296$, and the expected position of the CO(5–4) emission line is indicated by a black dotted line. The spectra are binned into $38.6\,\mathrm{km\,s^{-1}}$ channels. The best-fit Gaussian profile to the coadded spectrum is overlaid as a guide, scaled to the relative amplifications of the two images, and the velocities of the two brightest star-forming clumps measured by S09 are indicated by vertical lines. Each image shows positive flux at the systemic redshift of MS1358-arc, but individually they are only detected at $\sim 3\sigma$ significance.

Whilst the emission line centroid is extremely well-matched to the best-fit redshift of the nebular emission, the line is weak, highlighting the difficulty of these observations even with long integrations. We perform a number of tests to validate the robustness of the detection. First, we check how often a detection is made when coadding two random spectra from the original (non-coadded) cube. We generate 1000 combinations of two randomly-selected pixels on the map (excluding pixels which lie within one beam of MS1358-arc), then fit a Gaussian profile to the resulting coadded spectrum and compare this to a continuum-only fit. The probability of finding an emission line of equal significance to the target from two randomly-selected positions with a velocity centroid lying within $\pm 150 \mathrm{km\,s^{-1}}$ of the redshift of MS1358-arc and a line width in the range $\sigma = 30 - 250\,\mathrm{km\,s^{-1}}$ is 0.05%.

The CO(5–4) emission line we measure is centered at $z = 4.9297 \pm 0.0001$ with a line flux of $0.104 \pm 0.024\,\mathrm{Jy\,km\,s^{-1}}$ and Full Width at Zero Intensity of FWZI $= 150 \pm 20\,\mathrm{km\,s^{-1}}$, comparable to the velocity gradient measured across the source by S09. Error bars are obtained by fitting a Gaussian profile to the line and perturbing it in intensity, velocity and width to obtain a $\Delta\,\chi^2 = 1$ error surface, using a Monte Carlo routine with 10^5 realisations centered on the best fit.

We also construct a coadded channel map from the PdBI cube by extracting regions centered on the two images and co-adding them. The coadded cube is then spatially convolved with the PdBI beam, and spectrally convolved with a Gaussian with FWHM $= 100\,\mathrm{km\,s^{-1}}$. We estimate the noise at each spatial position using the off-line spectrum at that position, and divide the signal in the on-line slice of the convolved datacube by this noise map to construct a signal-to-noise map, shown in Figure 3. We find that 99.95% of the pixels have lower signal-to-noise than the target. This is equivalent to a detection significance of $3.5\,\sigma$.

In the following analysis, we treat the line flux as $0.104 \pm 0.024\,\mathrm{Jy\,km\,s^{-1}}$, but discuss the implications of treating it as an upper limit in Section 4.

3. Results, Analysis and Discussion

3.1. CO Dynamics, Luminosity and Molecular Gas Mass

Using the combined spectrum of Images 1 and 2, we first estimate the line luminosity and gas mass. Following Solomon & Vanden Bout (2005), the line luminosity is $L'_{\mathrm{CO(5-4)}} = (3.6 \pm 0.8) \times 10^9\,\mathrm{K\,km\,s^{-1}\,pc^2}$. Adopting a magnification factor of $\mu = 22 \pm 5$, this indicates an intrinsic $L'_{\mathrm{CO(5-4)}} = (1.6 \pm 0.5) \times 10^8\,\mathrm{K\,km\,s^{-1}\,pc^2}$.

To convert this CO(5–4) luminosity to a total molecular gas mass, we must first esti-

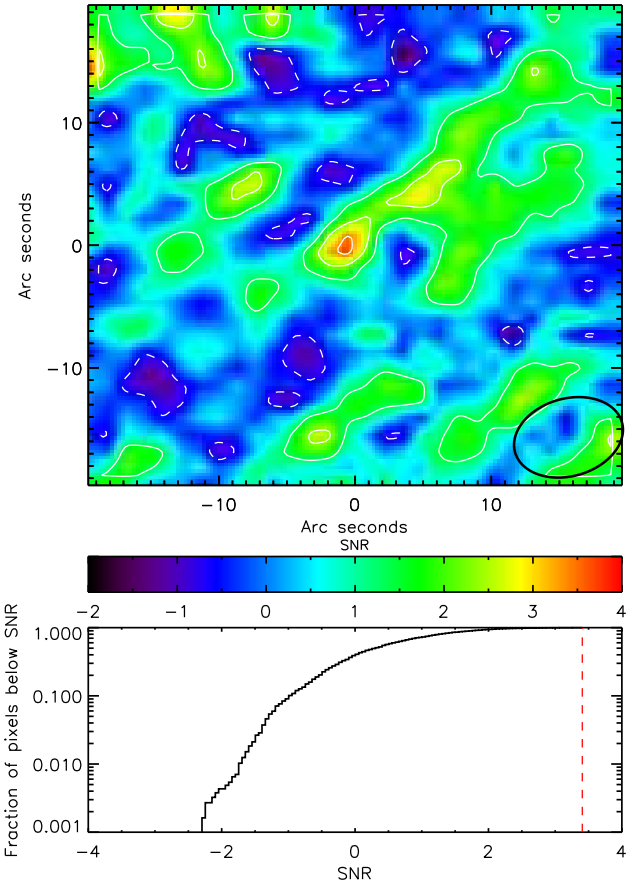

Fig. 3.— *Upper:* The coadded PdBI signal-to-noise channel map, constructed by extracting and coadding regions around each of the two images of MS1358-arc, convolved spatially with the beam and in the spectral direction with a Gaussian profile with FWHM= 100km s^{-1}, and then dividing each pixel by its noise. The combined image of the two targets is located in the centre of the map. The solid lines are intensity contours in $\pm 1\sigma$ intervals, with negative contours indicated by dashed lines. The beam size is indicated by the black ellipse line in the lower right-hand corner. *Lower:* Cumulative histogram of the signal-to-noise in the map, with the central pixel marked as a red dashed line. We find that just 0.05% of pixels have higher signal-to-noise than the emission seen from the source, suggesting a 3.5σ detection.

mate the corresponding CO(1–0) line luminosity. We therefore exploit recent observations of $z = 2 - 4$ galaxies where the ratio $L'_{\rm CO(5-4)}/L'_{\rm CO(1-0)}$ has been measured directly, e.g. $L_{\rm CO(5-4)}/L'_{\rm CO(1-0)} = 0.35 \pm 0.02$ for SMM J2135 (Danielson et al. 2011) or 0.32 ± 0.05 for a sample of SMGs (Bothwell et al. 2012). We adopt the latter value and applying it to MS1358-arc, we estimate $L'_{\rm CO(1-0)} = (5.0 \pm 1.7) \times 10^8\,{\rm K\,km\,s^1\,pc^2}$. If we instead assumed $L_{\rm CO(5-4)}/L'_{\rm CO(1-0)}$ from either the Antannae, 0.2 (Zhu et al. 2003); NGC 253, 0.7 (Bayet et al. 2004); or M 82, 0.7 (Weiß et al. 2005) this estimate would vary by a factor of 2× in either direction and so we adopt this as the likely systematic uncertainty in our estimate.

To derive the molecular gas mass $M_{\rm gas}$ from $L'_{\rm CO(1-0)}$, we assume $M_{\rm gas} = \alpha L'_{\rm CO(1-0)}$ where α is the coefficient relating the CO to H_2+He gas mass. We can derive an absolute lower limit for α by assuming that the molecular gas is enriched to solar metallicity and is optically thin to CO radiation. From Ivison et al. (2010), we have $\alpha \gtrsim 0.7$, which is consistent with the value $\alpha = 0.8$ applied to local (Ultra) Luminous InfraRed Galaxies ((U)LIRGs Solomon & Vanden Bout 2005). However, recent studies of high-z star-forming galaxies have suggested that $\alpha \sim 2$ may be a more appropriate conversion factor (e.g. Danielson et al. 2011; Ivison et al. 2011). Adopting this value, we find $M_{\rm gas} = 1^{+1}_{-0.6} \times 10^9\,{\rm M_\odot}$, where we conservatively estimate a factor of 2× uncertainty in α, comparable to the uncertainty in $L_{\rm CO(5-4)}/L'_{\rm CO(1-0)}$.

Combining our gas mass estimate with the stellar mass $M_* = 7 \pm 2 \times 10^8\,{\rm M_\odot}$ derived by S09, we obtain a total baryonic mass of $M_{\rm baryon} = M_* + M_{\rm gas} = 1.7^{+1.0}_{-0.6} \times 10^9{\rm M_\odot}$. This is consistent with the dynamical mass within 2kpc derived by S09 of $M_{\rm dyn} = 3 \pm 1 \times 10^9\,{\rm csc}^2(i)\,{\rm M_\odot}$, if the inclination is $i \gtrsim 45°$.

The gas fraction $f_{\rm gas} = M_{\rm gas}/\left(M_{\rm gas} + M_*\right)$ is typically $< 10\%$ in local large spiral galaxies (Young & Scoville 1991), or $\sim 33\%$ in local ULIRGs (Solomon et al. 1997). Other studies of molecular gas in high-redshift galaxies are beginning to find a trend for higher gas fractions at higher redshifts (Tacconi et al. 2010; Geach et al. 2011), which is in line with expectations from hydrodynamical simulations (Crain et al. 2009). For MS1358-arc, we find $f_{\rm gas} = 0.59^{+0.11}_{-0.06}$, with a systematic uncertainty of $\sim \pm 0.20$ due to α and $L_{\rm CO(5-4)}/L'_{\rm CO(1-0)}$.

In Figure 4, we compare the gas fraction of MS1358-arc to samples at lower redshift (see also Geach et al. 2011). The sample size is currently too small to draw any firm conclusions, and there are of course significant selection effects involved. We therefore caution that there are limits to the extent of any physical interpretation of this result, although it clearly motivates a uniformly-selected survey of the gas properties of high-redshift star-forming galaxies.

We can also use the dynamics of the [OII] emission to test whether the molecular gas is colocated with the star formation. In Figure 2, we overplot the redshifts of the two brightest star-forming knots, which are located at $\pm 150\,\mathrm{km\,s^{-1}}$ from the dynamical centre. Hence, if the CO gas traced the [OII] emission we would expect a FWZI of $\sim 300\mathrm{km\,s^{-1}}$, higher than the observed line width. This may indicate that the CO emission is associated with the dynamical centre of the galaxy rather than being concentrated in the star-forming regions or associated with the outflowing Lyα and UV-ISM lines (S09).

3.2. Gas depletion timescales

S09 derived a star formation rate (SFR) of $42 \pm 8\,\mathrm{M_\odot\,yr^{-1}}$ using the Kennicutt (1998) conversion from [OII] luminosity to SFR. We note that this conversion is consistent with the empirical correction to this calibration of Gilbank et al. (2010), which accounts for the metallicity dependence of the [OII]-derived SFR.

If MS1358-arc has sustained this SFR continuously, then the time taken to build up the current stellar mass of $7 \pm 2 \times 10^8\,\mathrm{M_\odot}$ is just $\tau_{\mathrm{build}} \sim 17$Myr (consistent with the age and star formation history used to derive the stellar mass). This suggests we may be seeing this galaxy in its first epoch of star formation. If this SFR is maintained at a constant level, the gas supply of $1 \times 10^9\,\mathrm{M_\odot}$ will be exhausted in $\sim 24\,\mathrm{Myr}$, which would place the galaxy $\sim 40\%$ of the way through its starburst. The star formation 'lifetime' of this galaxy would thus be very short compared to that inferred indirectly for the LBG population at $z = 4-6$, which have implied starburst lifetimes of $\lesssim 500\,\mathrm{Myr}$ (Stark et al. 2009), but is consistent with the lifetime of the starburst-triggered 'LBG phase' predicted by semi-analytic models (Gonzalez et al. 2011).

Finally, we note that the ratio between far-infrared luminosity and molecular gas mass, $L_{\mathrm{FIR}}/M_{\mathrm{H_2}}$, gives the star formation efficiency (SFE), relating the ongoing star formation to the available molecular gas.

Knudsen et al. (2008) obtained an upper limit on the $850\,\mu$m flux of MS1358-arc of $S_{850} < 4.8\,\mathrm{mJy}$ which, accounting for the lensing magnification and using the $S_{850} - L_{\mathrm{FIR}}$ calibration of Neri et al. (2003), suggests a far-infrared (FIR) luminosity $L_{\mathrm{FIR}} < 3.5 \times 10^{11}\,\mathrm{L_\odot}$ (we note that if we assume that the FIR flux is re-emitted light from dust-obscured star formation and apply the Kennicutt (1998) relation to our [OII]-derived SFR, we obtain $L_{\mathrm{FIR}} = (2.3 \pm 0.9) \times 10^{11}\,\mathrm{L_\odot}$, which is consistent with this upper limit). We thus obtain $SFE \lesssim 240\mathrm{L_\odot\,M_\odot^{-1}}$. For comparison, the median SFE in local ULIRGS is $49 \pm 6\,\mathrm{L_\odot\,M_\odot^{-1}}$ when corrected to $\alpha = 2$, although this rises to $172 \pm 23\mathrm{L_\odot\,M_\odot^{-1}}$ if $\alpha = 0.8$, which is the factor

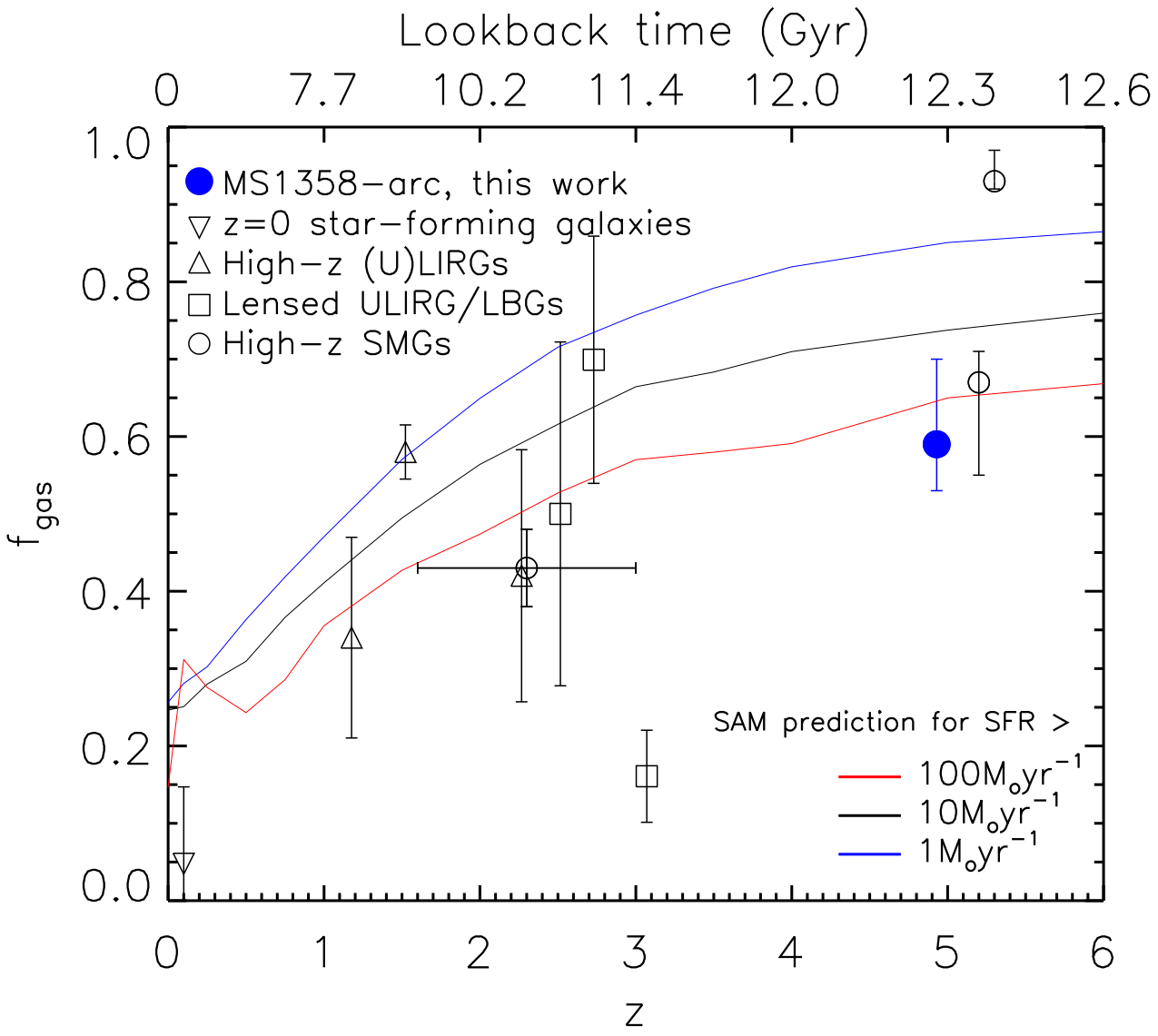

Fig. 4.— Evolution of the molecular gas fraction with redshift in star-forming galaxies. We compare MS1358-arc to the $z = 0$ sample of Leroy et al. (2008), the median gas fractions of the high-z LIRGs from Daddi et al. (2010a) and the median of each redshift bin of the Tacconi et al. (2010) (U)LIRG sample. We also use the lensed ULIRG from Kneib et al. (2005), lensed LBGs from Riechers et al. (2010a) and high-z SMGs from Bothwell et al. (2012), Riechers et al. (2010b) and Walter et al. (2012), all converted to $\alpha = 2$ for consistency. The lines are the predictions from semi-analytic models for galaxies with $SFR > 1, 10, 100\,\mathrm{M}_\odot\,\mathrm{yr}^{-1}$ (Lacey et al. in prep). From the limited data available, there is apparent evolution in the molecular gas fraction with redshift, broadly consistent with the semi-analytic models.

commonly applied to ULIRGs (Sanders et al. 1991), while SMGs give $SFE \sim 55^{+20}_{-15} \mathrm{L}_{\odot}\,\mathrm{M}_{\odot}^{-1}$ for $\alpha = 2$ (Bothwell et al. 2012). Our upper limit is consistent with these values.

4. Conclusions

We have used the IRAM Plateau de Bure Interferometer to search for the CO(5–4) emission in a $z = 4.9296$ galaxy lensed by the foreground cluster MS1358+62. We were able to observe two images of the galaxy simultaneously, with a total magnification factor of $22 \pm 5\times$. We measure a line flux of $0.104 \pm 0.024\,\mathrm{Jy\,km\,s^{-1}}$ at the position of the galaxy, yielding a detection at 3.5-4.3σ.

The molecular gas shows a relatively narrow velocity range around the systemic redshift, unlike the [OII] emission, which mainly arises from two clumps in the galaxy at $\pm 150\,\mathrm{km\,s^{-1}}$. This may suggest that the gas is more centrally concentrated than the star formation.

We derive a total gas mass $M_{\mathrm{gas}} = 1^{+1}_{-0.6} \times 10^9\,\mathrm{M}_{\odot}$, suggesting that this galaxy has a gas fraction $f_{\mathrm{gas}} = 0.59^{+0.11}_{-0.06}$, with a systematic uncertainty of $\sim \pm 0.20$ due to α and $L_{\mathrm{CO(5-4)}}/L'_{\mathrm{CO(1-0)}}$, which is similar to the most gas-rich galaxies at $z \sim 2$. This could imply that gas fractions do not continue to rise significantly beyond $z \sim 2$, though a larger sample is clearly needed to draw any conclusions.

Finally, given the tentative nature of the detection, we consider the implications of treating the measured flux as a 4σ upper limit. In this case, the resulting gas mass $M_{\mathrm{gas}} < 1 \times 10^9\,\mathrm{M}_{\odot}$ would be lower than expected given the stellar and dynamical masses derived by S09, and the gas fraction would be $f_{\mathrm{gas}} < 0.6$. This would also imply a gas depletion timescale of $< 24\,\mathrm{Myr}$, placing the galaxy more than 40% of the way through a short starburst.

Our observations highlight the difficulty of measuring gas properties of 'representative' star-forming galaxies at $z \sim 5$, an era when many of today's massive galaxies may be undergoing their first major episode of star formation. Probing their basic properties - their stellar and gas content and relation to star formation - will provide important physical quantities which galaxy formation models must reproduce.

The authors thank Malcolm Bremer, Seb Oliver and Isaac Roseboom for help and useful discussions. RCL acknowledges a studentship from STFC. AMS acknowledges an STFC Advanced Fellowship, and RGB, IRS and ACE acknowledge support from STFC. KEKC and JEG both acknowledge the support from NSERC. RAC is supported by the ARC. These observations were carried out with the IRAM Plateau de Bure Interferometer. IRAM is supported by INSU/CNRS (France), MPG (Germany) and IGN (Spain).

Facilities: IRAM:Interferometer.

REFERENCES

Baker, A. J., Tacconi, L. J., Genzel, R., Lehnert, M. D., & Lutz, D. 2004, ApJ, 604, 125

Bayet, E., Gerin, M., Phillips, T. G., & Contursi, A. 2004, A&A, 427, 45

Bothwell, M. S., Smail, I., Chapman, S. C., et al. 2012, ArXiv e-prints

Carilli, C. L., Daddi, E., Riechers, D., et al. 2010, ApJ, 714, 1407

Combes, F., Rex, M., Rawle, T. D., et al. 2012, A&A, 538, L4

Coppin, K. E. K., Chapman, S. C., Smail, I., et al. 2010, MNRAS, 407, L103

Coppin, K. E. K., Swinbank, A. M., Neri, R., et al. 2007, ApJ, 665, 936

Cox, P., Krips, M., Neri, R., et al. 2011, ApJ, 740, 63

Crain, R. A., Theuns, T., Dalla Vecchia, C., et al. 2009, MNRAS, 399, 1773

Daddi, E., Elbaz, D., Walter, F., et al. 2010a, ApJ, 714, L118

Daddi, E., Bournaud, F., Walter, F., et al. 2010b, ApJ, 713, 686

Danielson, A. L. R., Swinbank, A. M., Smail, I., et al. 2011, MNRAS, 410, 1687

Davies, L. J. M., Bremer, M. N., Stanway, E. R., Birkinshaw, M., & Lehnert, M. D. 2010, MNRAS, 408, L31

Förster Schreiber, N. M., Genzel, R., Bouché, N., et al. 2009, ApJ, 706, 1364

Franx, M., Illingworth, G. D., Kelson, D. D., van Dokkum, P. G., & Tran, K. 1997, ApJ, 486, L75

Geach, J. E., Smail, I., Moran, S. M., et al. 2011, ApJ, 730, L19+

Gilbank, D. G., Baldry, I. K., Balogh, M. L., Glazebrook, K., & Bower, R. G. 2010, MNRAS, 405, 2594

Gonzalez, J. E., Lacey, C. G., Baugh, C. M., Frenk, C. S., & Benson, A. J. 2011, ArXiv e-prints

Guilloteau, S., & Lucas, R. 2000, in Astronomical Society of the Pacific Conference Series, Vol. 217, Imaging at Radio through Submillimeter Wavelengths, ed. J. G. Mangum & S. J. E. Radford, 299

Guilloteau, S., Delannoy, J., Downes, D., et al. 1992, A&A, 262, 624

Ivison, R. J., Papadopoulos, P. P., Smail, I., et al. 2011, MNRAS, 46

Ivison, R. J., Smail, I., Papadopoulos, P. P., et al. 2010, MNRAS, 404, 198

Jullo, E., Kneib, J., Limousin, M., et al. 2007, New Journal of Physics, 9, 447

Kennicutt, Jr., R. C. 1998, ARA&A, 36, 189

Kneib, J. 1993, PhD thesis, Ph. D. thesis, Université Paul Sabatier, Toulouse, (1993)

Kneib, J., Neri, R., Smail, I., et al. 2005, A&A, 434, 819

Knudsen, K. K., van der Werf, P. P., & Kneib, J. 2008, MNRAS, 384, 1611

Law, D. R., Steidel, C. C., Erb, D. K., et al. 2009, ApJ, 697, 2057

Leroy, A. K., Walter, F., Brinks, E., et al. 2008, AJ, 136, 2782

McLure, R. J., Cirasuolo, M., Dunlop, J. S., Foucaud, S., & Almaini, O. 2009, MNRAS, 395, 2196

Neri, R., Genzel, R., Ivison, R. J., et al. 2003, ApJ, 597, L113

Ouchi, M., Shimasaku, K., Okamura, S., et al. 2004, ApJ, 611, 660

Richard, J., Stark, D. P., Ellis, R. S., et al. 2008, ApJ, 685, 705

Riechers, D. A., Carilli, C. L., Walter, F., & Momjian, E. 2010a, ApJ, 724, L153

Riechers, D. A., Hodge, J., Walter, F., Carilli, C. L., & Bertoldi, F. 2011a, ApJ, 739, L31

Riechers, D. A., Capak, P. L., Carilli, C. L., et al. 2010b, ApJ, 720, L131

Riechers, D. A., Cooray, A., Omont, A., et al. 2011b, ApJ, 733, L12+

Sanders, D. B., Scoville, N. Z., & Soifer, B. T. 1991, ApJ, 370, 158

Solomon, P. M., Downes, D., Radford, S. J. E., & Barrett, J. W. 1997, ApJ, 478, 144

Solomon, P. M., & Vanden Bout, P. A. 2005, ARA&A, 43, 677

Stanway, E. R., Bremer, M. N., Davies, L. J. M., et al. 2008, ApJ, 687, L1

Stark, D. P., Ellis, R. S., Bunker, A., et al. 2009, ApJ, 697, 1493

Stark, D. P., Ellis, R. S., Chiu, K., Ouchi, M., & Bunker, A. 2010, MNRAS, 408, 1628

Swinbank, A. M., Webb, T. M., Richard, J., et al. 2009, MNRAS, 400, 1121

Tacconi, L. J., Genzel, R., Neri, R., et al. 2010, Nature, 463, 781

Walter, F., Weiß, A., Riechers, D. A., et al. 2009, ApJ, 691, L1

Walter, F., Decarli, R., Carilli, C., et al. 2012, Nature, 486, 233

Weiß, A., Walter, F., & Scoville, N. Z. 2005, A&A, 438, 533

Young, J. S., & Scoville, N. Z. 1991, ARA&A, 29, 581

Zhu, M., Seaquist, E. R., & Kuno, N. 2003, ApJ, 588, 243